Finite Element Analysis for Dynamic Simulation of Composite HAWT Blade

Eslam Shamso *, Medhat El-Hadek*, Samar Elsanabary*
Abla El-Megharbel *‡, Rasha M. Soliman*

* Production Engineering and Mechanical Design Department, Faculty of Engineering, Port-Said University, 42523, Port-Said, Egypt

(eslam.shamso@eng.psu.edu.eg, melhadek@eng.psu.edu.eg, samar.abaas@eng.psu.edu.eg, aelmegharbel@eng.psu.edu.eg, rm.soliman@eng.psu.edu.eg)

‡ Corresponding Author; Abla El-Megharbel, Production Engineering and Mechanical Design Department, Faculty of Engineering, Port-Said University, 42523, Port-Said, Egypt, Tel: +20 1117529834, aelmegharbel@eng.psu.edu.eg

Received: xx.xx.xxxx Accepted:xx.xx.xxxx

Abstract- Wind turbines harvest wind energy and transform it into electricity every day, offering a sustainable energy source. The case study for this research was a HAWT (horizontal-axis wind turbine). General Electric's 1.5 MW series of HAWT was examined using a finite element FE modeling approach. The one-way connection was subjected to a fluid-mechanical, fluid-structural interaction (FSI) investigation. The maximum distortion energy theory may be used to determine the maximum value of stress on a HAWT, and total deformation at various speeds was discovered to be at 7, 10, 12, 15, and 20 m/s. Five composite materials were compared, including epoxy-S-glass, epoxy-E-glass, epoxy-carbon, Kevlar, and Technora. The obtained CFD results are compared with experimental data and the mathematical calculation of the GE 1.5-xle turbine. The experimental conducted by (NREL) results, and mode shape values agreed reasonably well. The results showed that an increase in wind speed caused an increase in blade deformation and von Mises stresses acting on the HAWT blade. Epoxy E Glass had the maximum deformation value of 833.49mm at 12m/s, while Kevlar had the minimum deformation value of 263.86mm at 12m/s. Kevlar also had the maximum von Mises stress value of 33.159MPa at 12m/s, while Epoxy E Glass had the minimum von Mises stress value of 27.695MPa at 12m/s.

Keywords Wind Turbine blade; Composite materials; ANSYS; Fluid-Structure Interaction; HAWT; Deformation; Stress.

NOMENCLATURE

Abbreviation			
FEA	Finite Element Analysis	C_D	Drag Coefficient
HAWT	Horizontal-Axis Wind Turbine	C_L	Lift Coefficient
GE	General Electric's	C_p	Power Coefficient
FSI	Fluid-Structural Interaction	α	Angle of Attack (°)
CFD	Computational Fluid Dynamic	ω	Angular Rotor Speed (rad/s)
BEM	Blade Element Momentum	v	Tangential Velocity (m/s)
NREL	National Renewable Energy Laboratory	R_r	Rotor Radius (m)
NACA	National Advisory Committee for Aeronautics	A	Projected Area (m)
		Ti	Turbulent intensity
		El	Element size (m)
Symbols		P_w	Power (MW)
F_L	lift force (N)	T	Torque (N.m)
F_D	Drag Force (N)	E	Young's Modulus (MPa)
F_R	Resultant Force (N)	**υ**	Poisson's Ratio
F_g	Gravitational Force (N)	**ρ**	Material Density (kg/m^3)
F_C	Centrifugal Forces (N)	m	Total Mass (kg)
F_r	Radial Force (N)	**σ**	Stress (MPa)
V_w	Speed of wind (m/s)	δ	Deformation (mm)

1. Introduction

Wind turbines are one of the most important renewable energy sources for extracting clean energy [1]. Wind energy generates well-paying jobs. Wind turbine service technicians are the second fastest-growing job in the United States, the wind industry has the potential to support hundreds of thousands more jobs by 2050 [1]. The aerodynamic analysis of horizontal-axis wind turbines HAWT is concerned with predicting rotor loads and energy production. Horizontal axis wind turbines are most seen in large-scale wind farms for national projects or industrial plants, their advantages make them the perfect solution for mass electricity production. Energy is a critical ingredient for commercial development and economic growth [2]. Renewable energy sources such as wind energy are naturally replenished and, thus, can help reduce the dependency on fossil fuels. Wind energy is the most important renewable energy resource [2]. Interactions between incompressible fluid flows and immersed structures are nonlinear multi-physics phenomena that have applications in a wide range of scientific and engineering disciplines. It discusses the challenges that researchers in this field face, as well as the importance of interdisciplinary collaboration in furthering the study of fluid-structure interactions [3]. Fluid-Structure Interaction (FSI) is a task of investigation for all design engineers and researchers. Therefore, proper FSI modeling is needed to meet the required standard for wind turbine development. FSI modeling requires the coupling of an aerodynamic (CFD) and a structural (FEA), allowing for aerodynamic and structural analysis of the studied model. Kyoungsoo. [4] performed experiments to obtain structural responses for the wind turbines at the national renewable energy laboratory NREL using ANSYS. The surface pressure information was imported from computational fluid dynamics CFD results. The new aerodynamic evaluation processes obtained the accuracy of the fluid-solid interaction FSI process using the CFD results. Munteanu. [5] presented the modal analysis of a wind turbine obtained via mathematical modeling. The blade model was designed using the CATIA software suite and imported into the ABAQUS suite. The modes and natural frequencies of the blade were modeled as a composite using glass fiber. The results proved natural frequencies were modified simultaneously while investigating the free and fixed structures. Khazem. [6] studied the stresses and deflection of a HAWT under the constant load condition; they also investigated the natural frequencies and mode shapes.The authors presented the stresses, total deformations, and the natural frequencies of HAWT; they found that the wind blade response improved when using the Al material instead of structural steel. Rajendra Roul. [7] presented stress analysis and displacements in composite materials for horizontal axis wind turbines HAWT 1.5 MW subjected to pressure obtained using the FSI one-way coupling with effect pitch angle. Michal Lipian. [8] studied the aerodynamic performance of a small wind turbine was investigated. The structural strength analysis of the prototype blades was performed as a one-way Fluid-Structure Interaction (FSI). Lambert. [9] studied fatigue cracks in wind turbines and the factors controlling these cracks. They analyzed the damage classification and the fatiguing part of the wind turbine blade materials. They explored the micromechanical damage processes of a wind turbine blade composite material. Lin Wang. [10] studied the fluid-structure interaction FSI model for HAWT; the aerodynamic loads were considered using computational fluid dynamics CFD applied in the ANSYS structural module and validated by a series of benchmark computational tests for the one-way FSI model. A parametric FEA (finite element analysis) model and a GA (genetic algorithm) model were used to create a structural optimization model for wind turbine composite blades [11]. E.Shamso. [12] present a complete analysis of fatigue life within a horizontal axis wind turbine blade HAWT under cyclic loads, and variable stresses have been investigated by using the Goodman theory. Rajaram.[13] present the vibration characteristics of the prototype horizontal axis wind turbine blade HAWT created with 3D modeling software. Karthikeyan. [14] present the low-velocity airfoil design and analysis solver XFOIL was used for numerical studies. The main objective of this research is to perform a structural analysis of HAWT blades made from composite materials using fluent and mechanical systems based on the FSI model. The HAWT blade is designed on the maximum deformation and stress values under effect FSI in one way. The stress analysis results were compared between dissimilar materials.

2. Benchmark and Validation of the FEA Model

Validation benchmarks involve calculations for the reliability of software coding and assessments of the numerical accuracy of the solution using a computational model [15,16]. The structural model of the blade was created using the FE approach with the structural modal workbench of ANSYS. The five-mode shapes consist of three flap-wise modes and two edgewise modes estimated from FEA, and the analysis results are shown in Table 1, Fig. 2, and Fig. 3. A mesh study was performed to find the optimum mesh size, considering the following five mesh sizes: 0.4 m,0.3 m, 0.2 m, 0.1 m, and 0.05 m, respectively, as shown in Fig. 1(a)-(e). The blade mode frequencies estimated from ANSYS were validated well with the FEA result of Lin Wang. and Sandia NuMAD blade [10,17] as shown in Fig. 2. The deviations in the numerical results decrease when the mesh element size is decreased; consequently, 0.2 m is the optimum mesh size, as shown in Table 1.

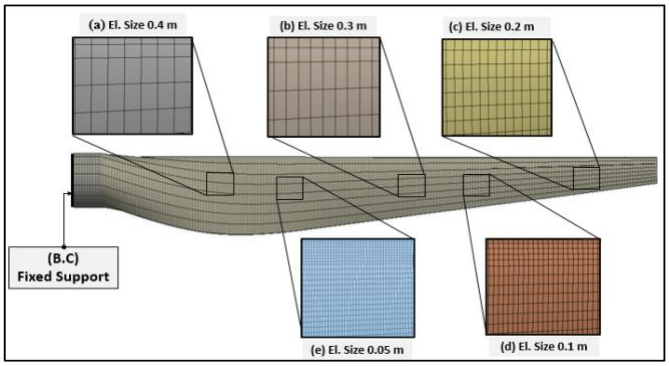

Fig. 1. The benchmark model boundary conditions and meshing with different element sizes (a) El. Size 0.4 m, (b) El. Size 0.3 m, (c) El. Size 0.2 m, (d) El. Size 0.1m, and(e) El. Size 0.05 m.

Table 1. Validation of the FEA model.

ID	*Mode frequencies (Hz)*	*Natural frequencies*						
		Sandia NuMAD blade[12]	*Lin Wang e al. [10]*	*ANSYS (mode shape) with different element size*				
				El. size 0.4m	*El. size 0.3m*	*El. size 0.2m*	*El. size 0.1m*	*El. size 0.05m*
				(a)	*(b)*	*(c)*	*(d)*	*(e)*
1	*1st flap-mode*	1.0783	1.0508	0.85961	0.86156	0.85786	0.86657	0.86711
2	*1st edge-mode*	1.7001	1.7003	1.5657	1.5642	1.5609	1.5468	1.5442
3	*2nd flap-mode*	2.9804	2.9329	2.4972	2.4985	2.4868	2.5045	2.5061
4	*2nd edge-mode*	5.0382	4.9672	5.3533	5.3546	5.3512	5.2908	5.2782
5	*3rd flap- mode*	6.3093	6.3978	5.9172	5.9136	5.9032	5.845	5.8335

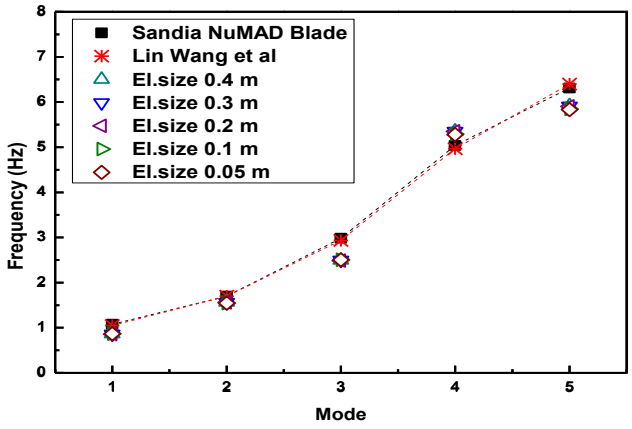

Fig. 2. Comparison of the frequency and mode shape for FEA validation.

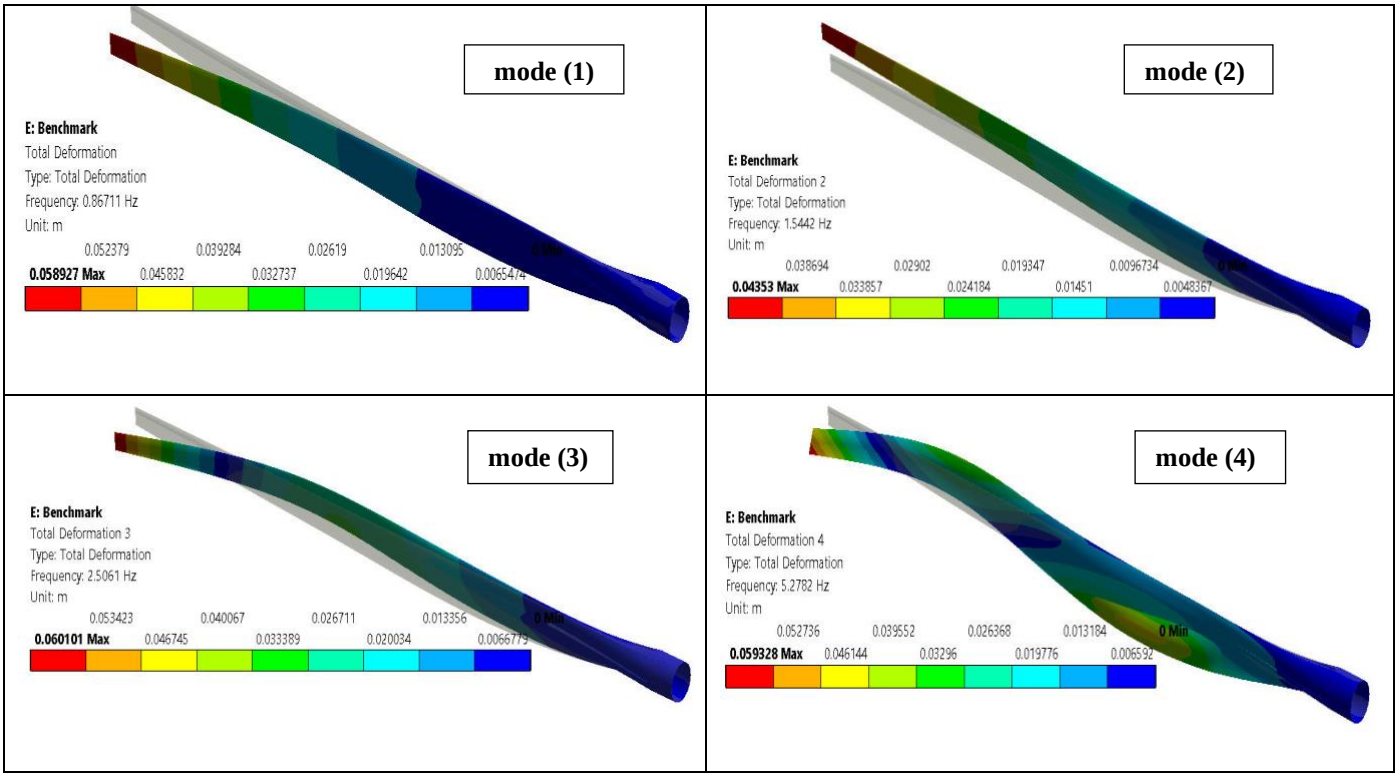

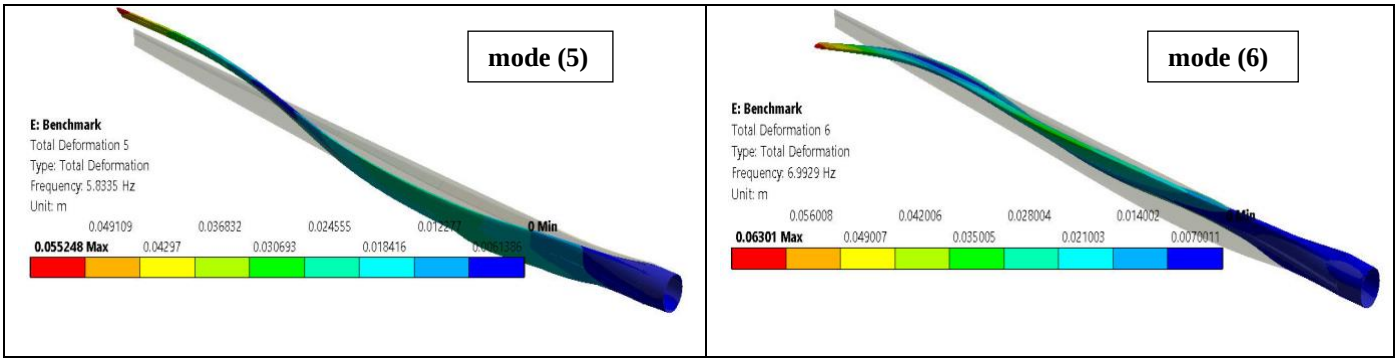

Fig. 3. Modal shapes of blade modes.

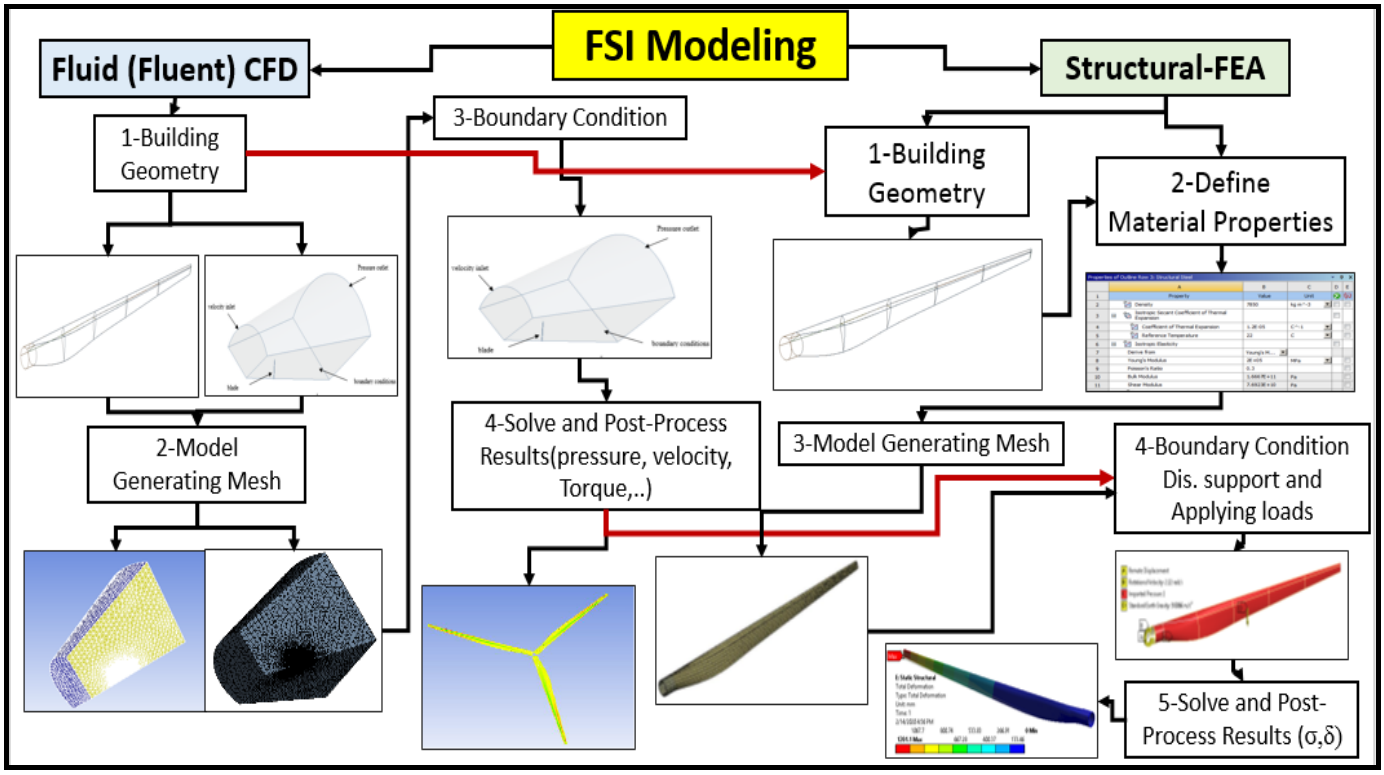

Fig. 4. Flowchart of CFD and FEA modeling.

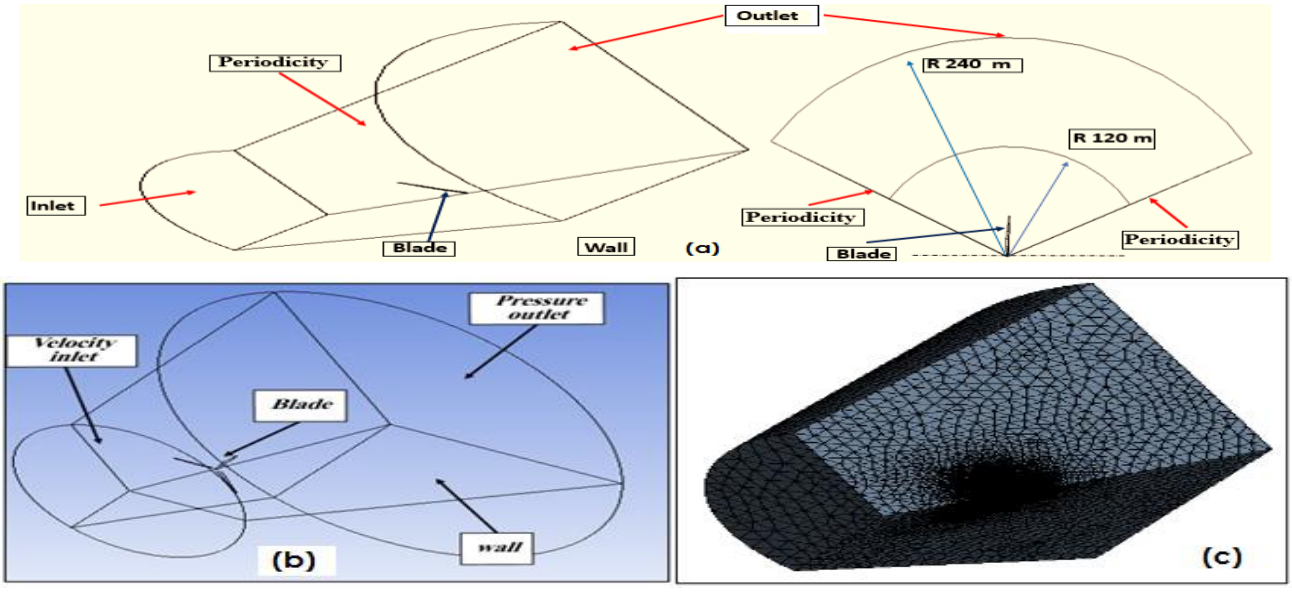

Fig. 5. Boundary conditions for (a)domain CFD modeling, (b) Full view of the domain, and (c) CFD mesh.

3. Methodology

The methodology consists of performing a structural analysis of HAWT blades made of composite materials using fluid-structural interaction systems based on the FSI model one-way coupling [18]. HAWT blade compared the stress and maximum deformation results between composite materials at different velocities. Figure 4 shows a flowchart of FSI modeling the complete fluid (fluent) CFD and structural-FEA coupling layout. For the design of the wind turbine model, meshing, boundary conditions, and post-processing results such as pressure and torque, CFD modeling is performed using the ANSYS Fluent software. On the other hand, structural FEA requires defining material properties, modeling meshes, defining boundary conditions, and solving stresses and deformations with different materials and velocities.

3.1 Loads on The Blade

The various types of wind turbine HAWT loads in Table 2 are aerodynamic, gravitational, and centrifugal [2,19]. The aerodynamic forces can be divided into aerodynamic loads such as the forces (the lift force F_L, the drag force F_D, and F_R is the resultant force) of the blades, as shown in Fig. 6. The aerodynamic force, gravitational loads F_g, and centrifugal loads F_c on the rotor are defined as shown in Table 2.

Table 2. The types of wind turbine loads.

Loads	*Equation*	
Aerodynamic Forces	$F_D = 0.5\rho C_D A V_w^2$	(1)
	$F_L = 0.5\rho C_L A V_w^2$	(2)
Gravitational Force	$F_{g\ rotor} = \sum_{i=1}^{n} m_i g$	(3)
Centrifugal Force	$F_c = \sum_{i=1}^{n} m_i r_i \omega^2$	(4)

In Table 2, F_D is the drag force; F_L is the lift force, C_D is the aerodynamic drag coefficient, C_L is the lift coefficient, A is the projected area vertical to the flow, and mi is the mass of the i-blade element. In addition, g = 9.82 m/s^2 , r_i is the radial position of the i-th blade element in the discretization of the blade into n elements, and ω is the angular rotor speed. As shown in Fig. 6, α is the angle of attack and F_R is the results force.

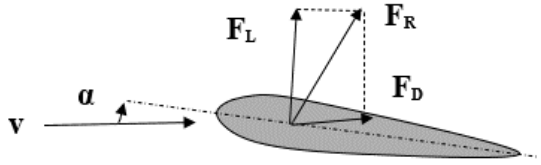

Fig. 6. Airfoil lift and drag.

3.2 Fluent CFD Modelling

3.2.1 Wind Turbine Blade Design

The wind turbine model used in this study is a 1.5-MW wind turbine, designed by National Renewable Energy Laboratory (NREL) [20,23]. General Electric's GE's 1.5MW series of HAWT is a GE renewable energy source fabricated in Germany. The rated power of the GE HAWT is 1.5 MW at a wind speed cut-in speed of 3.5 m/s, and the cut-out wind speed is 20 m/s [24,25]. The HAWT consists of three rotor blades. The 3D model of the HAWT was developed in SolidWorks and Design Modeler package software. The specifications of the 1.5MW wind turbines can be found in [7,22], and the main constraints are summarized in Table 3. The blade consists of three types of airfoils NACA S818, S825, and S826 [26], and one web. The 3D geometry is shown in Fig. 7.

Table 3. Wind turbine GE 1.5MW [7,22].

Parameters	***Values***	***Units***
Power	*1.5*	*MW*
Number of blades (N_B)	*3*	*Blade*
Airfoil (NACA)	*S818-S825-S826*	-
Rotor radius	*41.25*	*m*
Total area	*5346*	*m²*
Free stream velocity (V_w)	*7,10,12,15,20*	*m/s*
Rate rotor speed (ω)	*2.22*	*rad/s*
Air density	*1.225*	*kg/m^3*

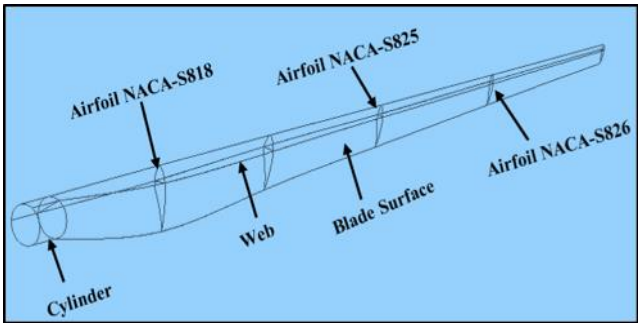

Fig. 7. Model HAWT of 1.5 MW.

3.2.2 B.C and Meshing of Fluent ANSYS Model

The fluent model of the blade is created using ANSYS computational fluid dynamics CFD simulation software Ansys fluent [27–29]. The computational domain, boundary conditions [4,7,10,30], as a symmetrical wind turbine rotates around its center of rotation, a single blade at 120^o radial stream tube field with rotating faces twice the solution can be used as shown in Fig. 5 [31,32], and the mesh used in the model fluent modeling are shown in Fig. 5-b The meshed wind turbine blade and domain

consist of 1896639 elements and 629768 nodes. The fluid domain's boundary conditions as shown in Table 4. General pressure-based continuity equations and material the fluid air density was 1.225 kg/m^3. The k-SST (shear-stress transport) model was used for this study [10,28]. Inlet different velocities 7,10,12,15, and 20 m/s, intensity, viscosity ratio 5% and 10, outlet pressure 1atm,no-slip blade, and periodic boundaries as shown in Table 4. The analysis results of the blade estimated from the fluent CFD model, such as pressure distribution, tangential velocity, and torque, show a good validation of the results.

Table 4. CFD boundary conditions.

No	***Boundary conditions.***
Inlet	- General =pressure-based - Wind velocity V_w= 7,10,12,15, and 20 m/s - Angular velocity =2.22 rad/s - Turbulent intensity T_I=5% - Viscosity ratio=10 - Material = air density 1.225 kg/m^3 - Model = k-SST
Outlet	- Pressure=1 atm
Side surface wall	- Rotational periodicity boundaries - No-slip

3.2.3 *Verification for Fluent Results*

Table 5 shows the percent of error between ANSYS and theoretical analysis for tangential velocity. Its rate was 2.07 %. Fig. 8 shows direction of the tangential velocity result.

$$Tangential\ velocity\ (v) = R_r \times \omega \qquad (5)$$

Where, ω: angular speed (rad/s), R_r: rotor radius (m), v: tip velocity (m/s).

Table 5. Comparative analysis of ANSYS result and the theoretical calculation.

ID	***Velocity (m/s)***	***Tangential velocity (m/s)***		***(%) Error***
		ANSYS	***Theoretical - calculation***	
1	*12*	*98.05*	*96.015*	*2.07*

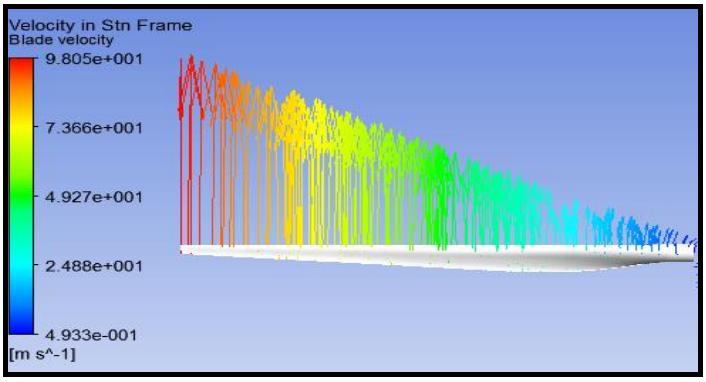

Fig. 8. Tangential velocity along the length.

3.2.4 *Pressure distributions*

Fig.9-(b) shows the pressure distributions and the wind velocities at 7, 10, 12, 15, and 20 m/s. Pressure contours on both the front and back sides of the blade are produced for each operational condition, as shown in Fig.9. In this case, the pressure side of the blade is designated as the upwind side, which is highly subjected to maximum pressure, and the back side is designated as the leeward side, which is subjected to negative pressure.

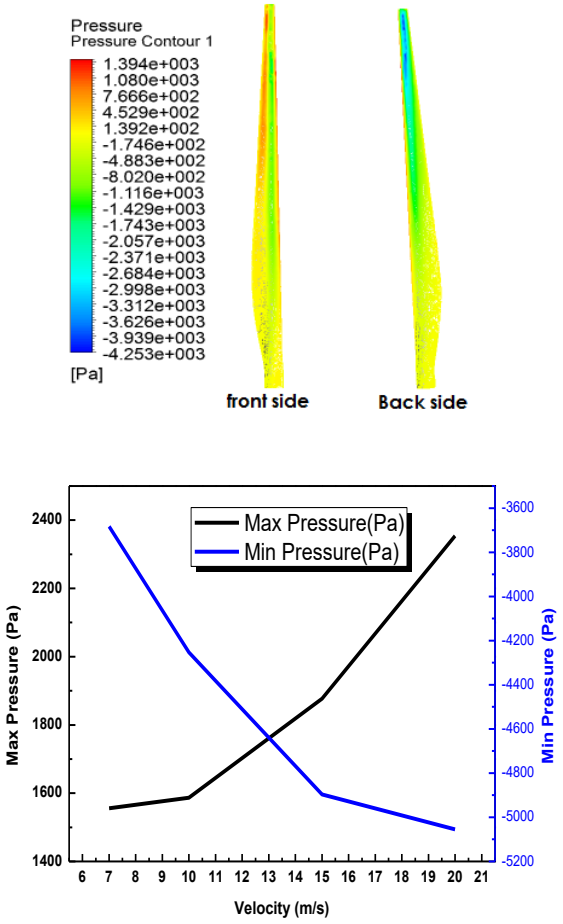

Fig.9: Pressure distributions of blade for different velocities.

3.2.5 Verification for Power and (Cp)

Table 6 shows the results for using the numerical ANSYS CFD results of the power coefficient with analytical calculations. The obtained CFD results are compared with the mathematical calculation and experimental data of the GE 1.5-xle turbine. There was a good agreement between power values and the results of experimental data. The results match well.

$$Power\ (P) = T \times \omega \quad (6)$$

$$C_P = \frac{P_{rated}}{P_{wind}} = \frac{P_{rated}}{0.5\rho A V^3} \quad (7)$$

Table 6. Comparison analysis of ANSYS result and the theoretical calculation.

ID	Parameter	Power - Power coefficient (C_p)			(%) Error
		Theoretical calculations	GE1.5MW-xle turbine	ANSYS CFD	
1	Cp	0.59	0.26	0.28	7.6%
2	Power	-	1.5	1.319	12%

3.3 Structural Analysis and Simulation Modelling

The finite element analysis FEA model was used in this study for a wind blade made of composite materials [16,33]. The commercial FE package ANSYS Workbench [28,34,35] was used to model HAWT using shell 181 elements [36]. FEA was used for CFD and FEA modelling by one-way FSI coupling [10]. This section presents the properties of the used composite materials, mesh element size, and boundary conditions for the FE model.

3.3.1 *Material Properties*

HAWT is made of composite materials to reduce the weight of these machines by simplifying the structural analysis by assuming that the isotropic material can approximate the composite material {Formatting Citation}. HAWT was manufactured with Epoxy-S-Glass, Epoxy-E-Glass, Epoxy-Carbon, Kevlar, and Technora [7]. In the analysis of the blade, these dissimilar materials were analysed. Table 7 gives a summary of the properties of these materials.

Table 7. Material properties of Elasticity [7].

Composite Material	E (GPa)	υ	ρ (kg/m³)
Epoxy-S-Glass	50	0.3	2000
Epoxy-E-Glass	45	0.3	2000
Epoxy-Carbon	121	0.27	1490
Kevlar	179	0.3	1470
Technora	70	0.3	1390

Where E is Young's modulus; υ is Poisson's ratio; *v* is the material density.

3.3.2 FE-Meshing

To create the structural model of the blade, using a mapping mesh method, the shell 181 element type [12,28,34]. In this study, the meshed wind turbine blade consisted of 14,445 elements and 14,130 nodes, with the smallest element size of 0.2 m, according to the benchmark. The meshing of the blade is shown in Fig. 10.

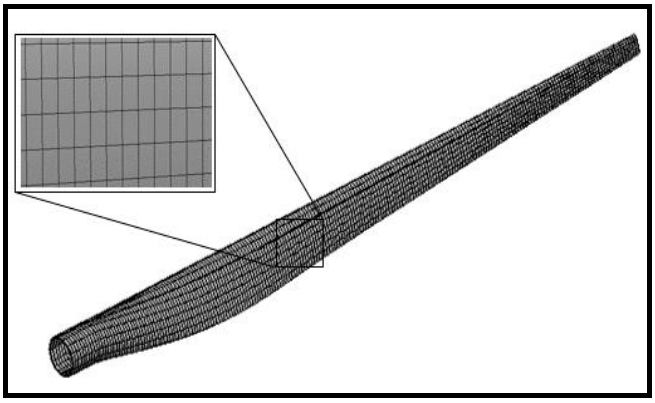

Fig. 10. FEA mesh of the blade.

3.3. 3 B.C for Fluid-Structural Interaction Modelling

To create the structural model of the blade. In addition to aerodynamic loads, other important forces were acting on the blades, such as gravity and centrifugal loads. The blade model was fixed support from the root presented in Fig. 11. the pressure was imported from the fluent analysis to the structural analysis. A variable pressure was distributed over the blade's surface, as shown in Fig. 11.

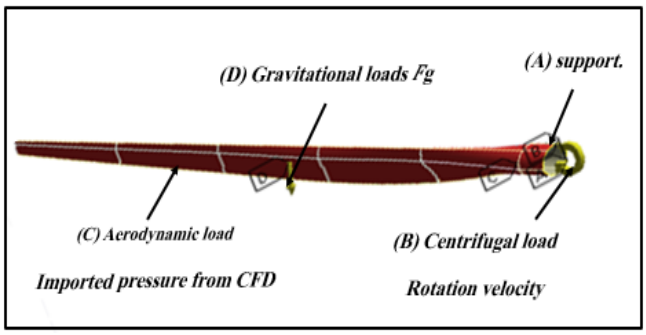

Fig. 11. Boundary conditions of the blade.

3.3.4 Post-Processing Results

FE analysis was used for fluent-mechanical coupling, and the pressure was determined using the fluent system CFD. The maximum stress value was determined using the distortion energy theory given by von Mises. The ANSYS package determined deformation at different velocities of 7, 10, 12, 15, and 20 m/s.

4. Results and Discussion

In this study, the rotor blades were made from different composite materials. Comparing the stress analysis results for the five materials on FSI, total deformation, and equivalent von Mises stresses.

4.1 Verification for Structural Results

Table 8 and Fig. 12 show the results for using the numerical ANSYS results of radial force with analytical calculations. The analysis results were compared between different composite materials. There was a good agreement between radial force values and the results of analytical calculations. The results match very well.

$$Radial\ Force\ (F) = -m\ r\ \omega^2 \quad (8)$$

Where; m: total mass (kg), ω: angular speed (rad/s).

Table 8. Comparison of the radial force between ANSYS and analytics calculations for different composite materials at 12 m/s.

ID	Composite Materials	At Vw =12 (m/s) Radial Force (KN)		(%) Error
		ANSYS	Analytical-Calculations	
1	Glass-S	2.0225×10^3	2.0339×10^3	0.563
2	Glass-E	2.0226×10^3	2.0339×10^3	0.558
3	Carbon-Epoxy	1.5076×10^3	1.5152×10^3	0.504
4	Kevlar	1.4874×10^3	1.4949×10^3	0.504
5	Technora	1.4067×10^3	1.4136×10^3	0.490

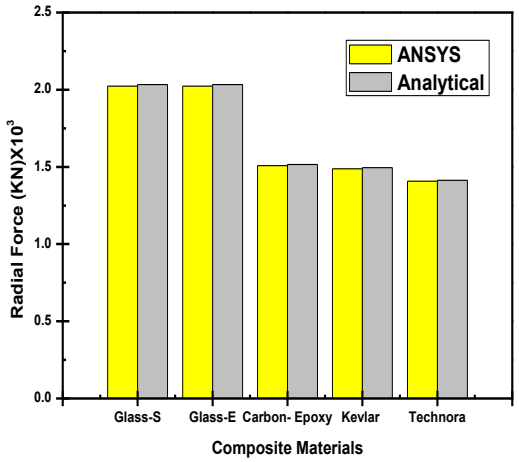

Fig. 12. Comparison of the radial force between ANSYS and Analytical.

4.2 Stresses and Deformation

4.2.1 Von Mises Stresses

Fig. 13 shows the stresses and wind velocities in the five composite materials, namely, Epoxy S-Glass and Epoxy E-Glass, Epoxy-Carbon, Kevlar, and Technora, from 7 to 20 m/s. The stresses of Epoxy S-Glass and Epoxy E-Glass showed a steady but significant rise over the period. For a velocity of 12 m/s, the graphs of the different composite materials show stresses of approximately 28.329MPa, 27.695MPa, 32.304MPa, 33.159MPa, and 30.582MPa, respectively. The comparative analysis of the ANSYS results of different materials and the stresses are shown in Fig. 13, Fig. 15, and Table 9.

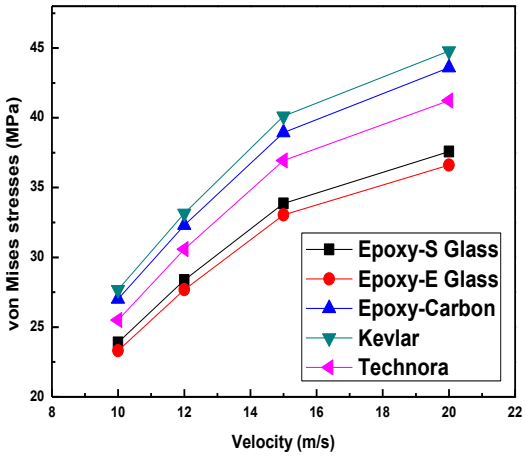

Fig. 13. Comparative analysis of ANSYS results for von Mises stresses.

Table 9 shows a comparative analysis of ANSYS results for the stresses at different wind velocities. The five velocities of HAWT were estimated, and the analysis results were. The results thoroughly analysis value, as illustrated in Fig. 15, due to FSI one-way coupling for HAWT.

4.2.2 Deformation

Fig. 14 shows the deformation and the wind velocities in composite materials, Epoxy S-Glass and Epoxy E-Glass, Epoxy-Carbon, Kevlar, and Technora, for velocities ranging from 7 to 20 m/s. The deformation of five composite materials increased sharply throughout the period. They determine the maximum deformation for materials with a value of767.59mm,833.49mm,379.78mm, 263.86mm, and 629.44mm at 12m/s.

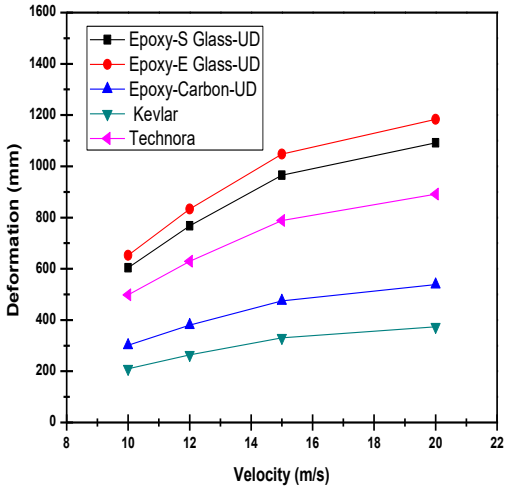

Fig. 14. Comparative analysis of ANSYS results for the deformation and wind velocity.

Table 9. Comparative analysis of ANSYS results for stresses at different wind velocities.

ID	Velocity (m/s)	ANSYS Result (Stresses von Mises (MPa)) with different Composite Materials				
		Epoxy-S Glass	Epoxy-E Glass	Epoxy-Carbon	Kevlar	Technora
1	7	19.949	19.951	18.042	18.404	17.146
2	10	23.893	23.308	27.014	27.677	25.497
3	12	28.329	27.69	32.304	33.159	30.582
4	15	33.857	33.04	38.947	40.117	36.936
5	20	37.575	36.617	43.586	44.794	41.236

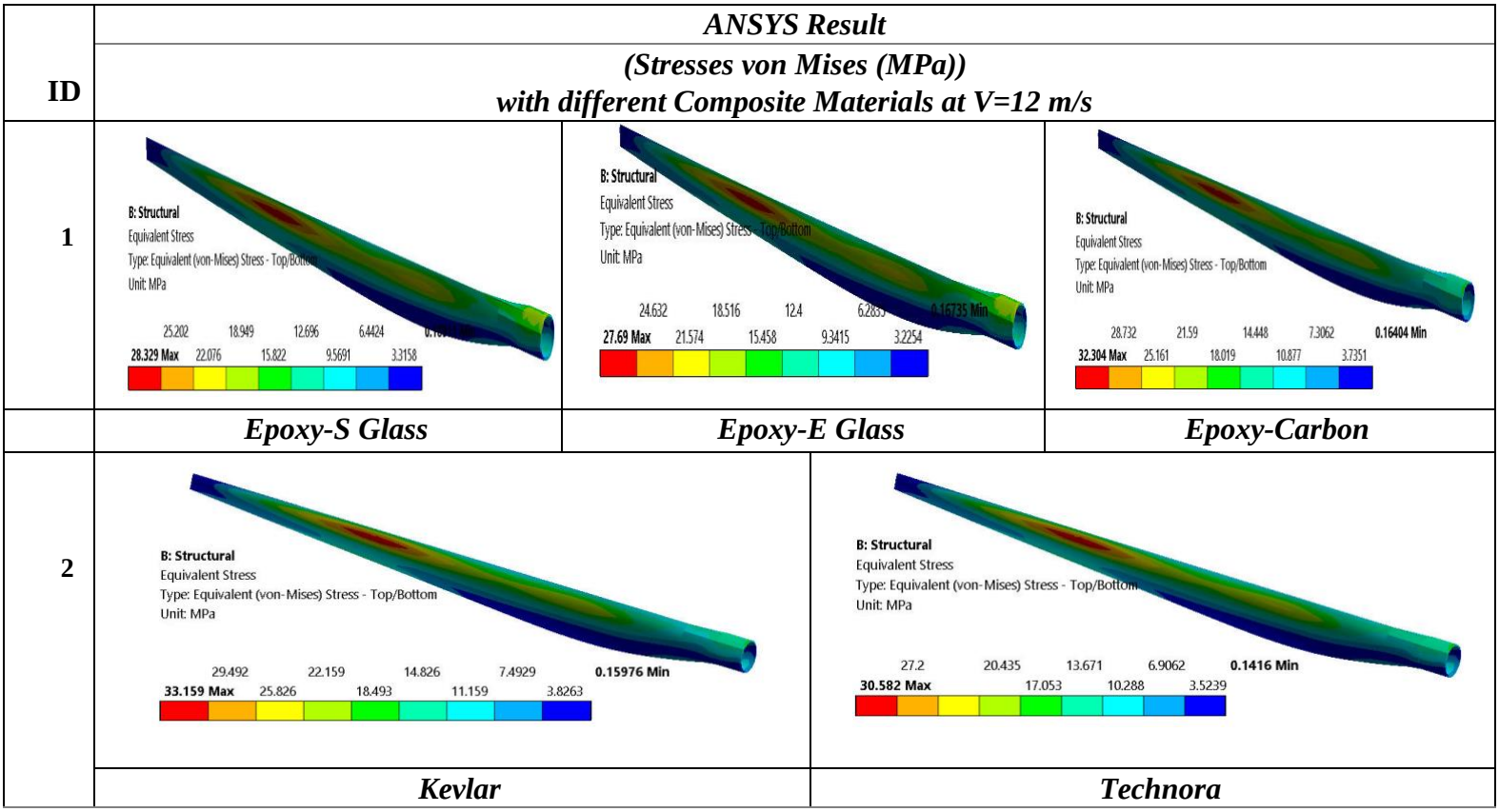

Fig. 15. Result for different Composite Materials at V_w=12 m/s for Max stresses.

Table 10 shows a comparative analysis of ANSYS results for the deformation at different wind velocities and the analysis results. The results completely analysis value, as illustrated in Fig. 16, due to FSI one-way coupling for HAWT.

5. Conclusions

FEA was used to study the complex shape of a wind turbine blade of 1.5MW made of composite materials; Epoxy E Glass, Epoxy S Glass, Epoxy-Carbon, Kevlar, and Technora at different wind velocities, and turbine blades were successfully modelled. Based on the results obtained, the following observations can be reported:

The benchmark data showed that the results from the operation of the model were able to solve the model form of the HAWT and the best mesh size was 0.2 m. A good agreement in their mode shapes natural frequencies for the HAWT of 1.5MW, and the experiment results were validated with the results given by Lin Wang et al. and Sandia NuMAD blade.

Table 10. Comparative analysis of ANSYS results for the deformation at different wind velocities.

ID	Velocity (m/s)	ANSYS Result (Max Deformation (mm)) with different Composite Materials				
		Epoxy-S-Glass	Epoxy-E-Glass	Epoxy-Carbon	Kevlar	Technora
1	7	344.32	374.55	170.23	118.19	283.54
2	10	604.05	652.89	301.84	209.61	498.21
3	12	767.59	833.49	379.78	263.86	629.44
4	15	965.32	1047.2	474.78	330.72	788.43
5	20	1092.1	1183.1	538.66	373.81	891.34

ID	ANSYS Result (Max deformation (mm)) with different Composite Materials at V=12 m/s		
1	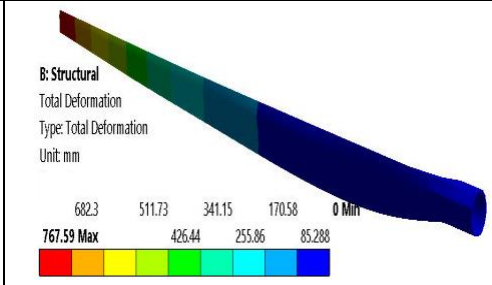	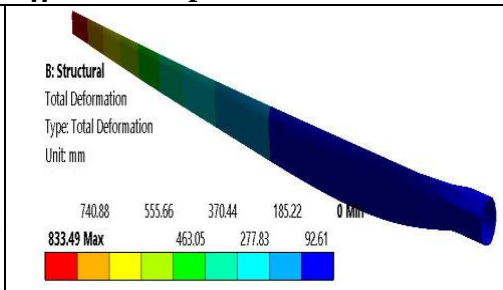	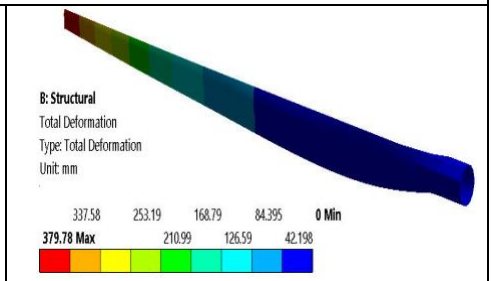
	(a)Epoxy-S Glass	*(b)Epoxy-E Glass*	*(c)Epoxy-Carbon*
2	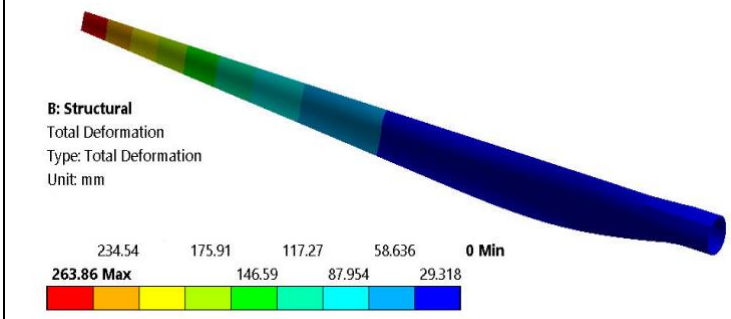	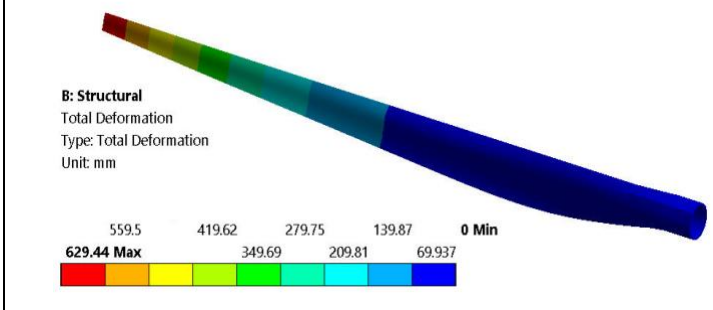	
	(d)Kevlar	*(e)Technora*	

Fig. 16. Result for different Composite Materials at V_w=12 m/s for Max Deformation**.**

The blade velocity from the analytical calculations is 96.015m/s, and from the CFD analysis, it is 98.05m/s. There was a good agreement between the radial force values and the results of the analytical calculations. The obtained CFD results are compared with experimental data and the mathematical calculation of the GE 1.5 xle turbine. The increase in the wind speed causes an increase in the blade deformation, and von Mises stresses acting on the HAWT blade. The maximum deformation was achieved using Epoxy E Glass with a value of 833.49mm at 12m/s. The minimum deformation, with a value of 2363.86mm at 12m/s, was used by Kevlar. The maximum stress blade von Mises stresses for Kevlar is 33.159MPa at a speed of 12 m/s. At 12 m/s, the minimum blade von Mises stresses for Epoxy E Glass are 27.695 MPa. The maximum deformation at the blade for Epoxy S Glass, Epoxy E Glass, Epoxy-Carbon, Kevlar, and Technora are 767.59mm, 833.49mm, 379.78mm, 263.86mm, and 629.44mm at 12m/s. The cause for this is that Kevlar has good strength. The maximum stresses for Epoxy S Glass, Epoxy E Glass, Epoxy-Carbon, Kevlar, and Technora are 28.329MPa, 27.695MPa, 32.304MPa, 33.159MPa, and 30.582MPa at 12m/s, respectively. This paper provides valuable insights into the use of FEA to analyze wind turbine blades and the performance of different composite materials used in their construction. These results can be used to improve the design and development of wind turbines, leading to more efficient and durable structures.

Funding: This is self-supported research without funding from any agency whatsoever.

Conflicts of Interest: The authors declare that there is no conflict of interest regarding the publication of this paper.

Reference

[1] A.A.S. Moussa, Wind Energy In Egypt, DEWI Mag. Nr 17, August 2000. (2000) 55–57.

[2] M.O.L. Hansen, Aerodynamics Of Wind Turbines, 2008.

[3] G. Hou, J. Wang, A. Layton, Numerical Methods For Fluid-Structure Interaction - A Review, Commun. Comput. Phys. 12 (2012) 337–377. Https://Doi.Org/10.4208/Cicp.291210.290411s.

[4] K. Lee, Z. Huque, R. Kommalapati, S.E. Han, Fluid-Structure Interaction Analysis Of NREL Phase VI Wind Turbine: Aerodynamic Force Evaluation And Structural Analysis Using FSI Analysis, Renew. Energy. 113 (2017) 512–531. Https://Doi.Org/10.1016/J.Renene.2017.02.071.

[5] M. V. Munteanu, M.D. Stanciu, S.M. Năstac, A. Savin, Modal Analysis Of Small Turbine Blade Made From Glass Fibres Composites, IOP Conf. Ser. Mater. Sci. Eng. 444 (2018). Https://Doi.Org/10.1088/1757899X/444/6/062004.

[6] E.A.Z. Khazem, O.I. Abdullah, L.A. Sabri, Steady-State And Vibration Analysis Of A Windpact 1.5-MW Turbine Blade, FME Trans. 47 (2019)195–201. Https://Doi.Org/10.5937/Fmet1901195k.

[7] R. Roul, A. Kumar, Fluid-Structure Interaction Of Wind Turbine Blade Using Four Different Materials: Numerical Investigation, Symmetry (Basel).12(2020). Https://Doi.Org/10.3390/Sym12091467.

[8] M. Lipian, P. Czapski, D. Obidowski, Fluid-Structure Interaction Numerical Analysis Of A Small, Urban Wind Turbine Blade, Energies. 13 (2020)1–15. Https://Doi.Org/10.3390/En13071832.

[9] J. Lambert, A.R. Chambers, I. Sinclair, S.M. Spearing, Damage Characterisation And The Role Of Voids In, (N.D.) 1–6.

[10] L. Wang, R. Quant, A. Kolios, Fluid Structure Interaction Modelling Of Horizontal-Axis Wind Turbine Blades Based On CFD And FEA, J. Wind Eng. Ind. Aerodyn. 158 (2016) 11–25. Https://Doi.Org/10.1016/J.Jweia.2016.09.006.

[11] L. Wang, A. Kolios, T. Nishino, P.L. Delafin, T. Bird, Structural Optimisation Of Vertical-Axis Wind Turbine Composite Blades Based On Finite Element Analysis And Genetic Algorithm, Compos. Struct. 153 (2016) 123–138. Https://Doi.Org/10.1016/J.Compstruct.2016.06.003.

[12] E. Shamso, M. Elhadek, G. Osmun, A. El-Megharbel, Fatigue Cycling Of NACA 821 Blades In Horizontal Wind Turbines, SYLWAN. (2019) 79–99.

[13] M. Rajaram Narayanan, S. Nallusamy, Analysis On Vibration Characteristics Of Wind Turbine Blade To Improve The Effectiveness Through Cfd Developed By Ansys, Mater. Sci. Forum. 937 MSF(2018)43–50. Https://Doi.Org/10.4028/Www.Scientific.Net/MSF.937.43.

[14] K. Natarajan, T. Suthakar, Insight Aerodynamic Analysis On Small-Scale Wind Turbines Airfoils For Low Reynolds Number Applications, Environ. Prog. Sustain. Energy. 41 (2022). Https://Doi.Org/10.1002/Ep.13807.

[15] S.Timoshenko -Strength Of Materials_ Elementary Theory And Problems - Vol. I-CBS (1 December 200).Pdf, N.D.

[16] M.A. El-Hadek, Dynamic Equivalence Of Ultrasonic Stress Wave Propagation In Solids, Ultrasonics.83(2018)214–221. Https://Doi.Org/10.1016/J.Ultras.2017.06.007.

[17] B.R. Resor, J. Paquette, Printed October 2012 A Numad Model Of The Sandia TX-100 Blade, (2012).

[18] F.K. Benra, H.J. Dohmen, J. Pei, S. Schuster, B. Wan, A Comparison Of One-Way And Two-Way

Coupling Methods For Numerical Analysis Of Fluid-Structure Interactions, J. Appl. Math. 2011 (2011). Https://Doi.Org/10.1155/2011/853560.

[19] G. Ingram, Wind Turbine Blade Analysis Using The Blade Element Momentum Method., October.1.1(2011)1–21. Https://Community.Dur.Ac.Uk/G.L.Ingram/Download/Wind_Turbine_Design.Pdf.

[20] T.C.E.T.Cest,Unsteady Aerodynamics Experiment Phase VI: Wind Tunnel Test Configurations And Available Data Campaigns, (2017) 27–28.

[21] J.M. Jonkman, M.L. Buhl Jr, FAST User's Guide 2005, Contract. (2005).

[22] P.J. Schubel, R.J. Crossley, Wind Turbine Blade Design, Wind Turbine Technol. Princ. Des. (2014) 1–34. Https://Doi.Org/10.1201/B16587.

[23] D.M. Somers, The S829 Airfoil Period Of Performance : 1994 – 1995 The S829 Airfoil, (2005) 1994–1995.

[24] E. Herter, Wind Turbine., (1979).

[25] Https://En.Wind-Turbine Models.Com/Turbines/656-Ge-General-Electric-Ge-1.5xle, (N.D.). [Accessed 20 March 2023]

[26] Airfoiltools,(N.D.). Http://Airfoiltools.Com/Airfoil/Details?Airfoil=S818-Nr. [Accessed 20 March 2023].

[27] Ansys Inc., Ansys Fluent 14.0 Tutorial Guide, Ansys Inc. 15317 (2009) 724–746.

[28] Fluent, Ansys, Ansys Fluent 16.0 Theory Guide, (2016).

[29] Fluent, Ansys. "Ansys Fluent 12.0 Theory Guide." Ansys Inc., Canonsburg, Pa (2009)., (N.D.).

[30] M.B. Farghaly, E.S. Abdelghany, Study The Effect Of Trailing Edge Flap Deflection On Horizontal Axis Wind Turbine Performance Using Computational Investigation, Int. J. Renew. Energy Res. 12 (2022) 1942–1953. Https://Doi.Org/10.20508/Ijrer.V12i4.13433.G8617.

[31] K. Osintsev, S. Aliukov,A.Shishkov, Improvement Dependability Of Offshore Horizontal-Axis Wind Turbines By Applying New Mathematical Methods For Calculation The Excess Speed In Case Of Wind Gusts, Energies. 14 (2021). Https://Doi.Org/10.3390/En14113085.

[32] N.A. Mezaal, K. V. Osintsev, S. V. Alyukov, The Computational Fluid Dynamics Performance Analysis Of Horizontal Axis Wind Turbine, Int. J. Power Electron. Drive Syst. 10 (2019) 1072–1080. Https://Doi.Org/10.11591/Ijpeds.V10.I2.1072-1080.

[33] E.H. Dill, The Finite Element Method For Mechanics Of Solids With Ansys Applications, 2011. Https://Doi.Org/10.1201/B11455.

[34] X. Chen, Y. Liu, Finite Element Modeling And Simulation With Ansys Workbench, 2014. Https://Doi.Org/10.1201/B17284.

[35] S. Moaveni, Finite Element Analysis Theory And ApplicationWithAnsys,2007.

[36] Ansys, Ansys Workbench Release 10.0, Ansys Work.Release10.0.(2005).Http://Kashanu.Ac.Ir/Files/Content/AnsysWorkbench.Pdf.

[37] B. Benbouhenni, "Application of STA Methods and Modified SVM Strategy in Direct Vector Control System of ASG Integrated to Dual-Rotor Wind Power: Simulation Studies", International Journal of Smart Grid, Vol. 5, No. 1, pp. 63-67, 2021.

[38] M.H. Rady, R.K. Garmode, M. Gooroochurn, S.A. Kale, Effect of Blade Root Dimensions on Physical and Mechanical Characteristics of a Small Wind Turbine Blade, Int. J. Renew. Energy Res.12(2022)1339–1346. https://Doi.org/10.20508/ijrer.v12i3.13283.g8518.

[39] R. Soto-Valle, S. Bartholomay, M. Manolesos, C. N. Nayeri and C. Oliver Paschereit, "On the Influence of trip strips on Rotor Blade Measurements," 2020 9th International Conference on Renewable Energy Research and Application, 2020,pp.188-195, https://Doi:10.1109/ICRERA49962.2020.9242848.

[40] M. Colak, I. Cetinbas and M. Demirtas, "Fuzzy Logic and Artificial Neural Network Based Grid-Interactive Systems for Renewable Energy Sources: A Review," 2021 9th International Conference on Smart Grid (icSmartGrid), 2021, pp.186-191. Doi:https://10.1109/icSmartGrid52357.2021.9551219.